ACCOUNTS
of chemical research

Synthetic Ion Transporters that Work with Anion−π Interactions, Halogen Bonds, and Anion−Macrodipole Interactions

ANDREAS VARGAS JENTZSCH, ANDREAS HENNIG,
JIRI MAREDA, AND STEFAN MATILE*
Department of Organic Chemistry, University of Geneva, Geneva, Switzerland

RECEIVED ON JANUARY 20, 2013

CONSPECTUS

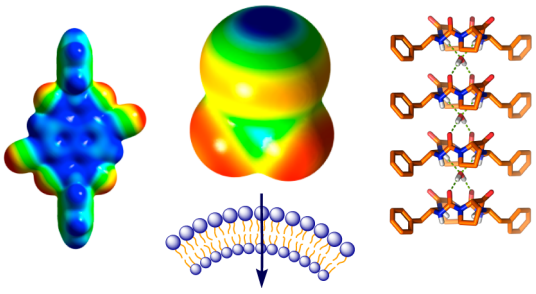

The transport of ions and molecules across lipid bilayer membranes connects cells and cellular compartments with their environment. This biological process is central to a host of functions including signal transduction in neurons and the olfactory and gustatory sensing systems, the translocation of biosynthetic intermediates and products, and the uptake of nutrients, drugs, and probes. Biological transport systems are highly regulated and selectively respond to a broad range of physical and chemical stimulation. A large percentage of today's drugs and many antimicrobial or antifungal agents take advantage of these systems. Other biological transport systems are highly toxic, such as the anthrax toxin or melittin from bee venom.

For more than three decades, organic and supramolecular chemists have been interested in developing new transport systems. Over time, curiosity about the basic design has evolved toward developing of responsive systems with applications in materials sciences and medicine. Our early contributions to this field focused on the introduction of new structural motifs with emphasis on rigid-rod scaffolds, artificial β-barrels, or π-stacks. Using these scaffolds, we have constructed selective systems that respond to voltage, pH, ligands, inhibitors, or light (multifunctional photosystems). We have described sensing applications that cover the three primary principles of sensor development: immunosensors that use aptamers, biosensors (an "artificial" tongue), and differential sensors (an "artificial" nose).

In this Account, we focus on our recent interest in applying synthetic transport systems as analytical tools to identify the functional relevance of less common noncovalent interactions, anion−π interactions, halogen bonds, and anion−macrodipole interactions. Anion−π interactions, the poorly explored counterpart of cation−π interactions, occur in aromatic systems with a positive quadrupole moment, such as TNT or hexafluorobenzene. To observe these elusive interactions in action, we synthesized naphthalenediimide transporters of increasing π-acidity up to an unprecedented quadrupole moment of +39 Buckinghams and characterized these systems in comparison with tandem mass spectrometry and computational simulations. With π-acidic calixarenes and calixpyrroles, we have validated our results on anion−π interactions and initiated our studies of halogen bonds. Halogen bonds originate from the σ-hole that appears on top of electron-deficient iodines, bromines, and chlorines. Halogen-bond donors are ideal for anion transport because they are as strong and at least as directional as hydrogen-bond donors, but also hydrophobic. The discovery of the smallest possible organic anion transporter, trifluoroiodomethane, illustrates the power of halogen-bond donors. This molecule contains a single carbon atom and is a gas with a boiling point of −22 °C. Anion−macrodipole interactions, finally, differ significantly from anion−π interactions and halogen bonds because they are important in nature and cannot be studied with small molecules. We have used anion-transporting peptide/urea nanotubes to examine these interactions in synthetic transport systems. To facilitate the understanding of the described results, we also include an in-depth discussion of the meaning of Hill coefficients.

The use of synthetic transport systems to catch less common noncovalent interactions at work is important because it helps to expand the collection of interactions available to create functional systems. Progress in this direction furthers fundamental knowledge and invites many different applications. For illustration, we briefly discuss how this knowledge could apply to the development of new catalysts.

Published on the Web 04/02/2013 www.pubs.acs.org/accounts
10.1021/ar400014r

1. Introduction

Since its inception in the late 1970s, research on synthetic transport systems has grown into a mature field. Progress is being reviewed regularly.[1−8] These reviews put increasing emphasis on subdomains because full coverage of the expanding field is becoming increasingly difficult. However, this special issue will produce a comprehensive summary of the state of the art in the broadest sense.[9] Given this unique situation, we felt that a more general introduction would be redundant and decided to entirely focus on our own contributions to the field.

The first contribution to the field was the introduction of rigid-rod molecules as membrane-spanning scaffolds.[10] This idea worked out very well. Depth quenching experiments demonstrated that rigid-rod scaffolds of a length that matches the thickness of lipid bilayer membranes adopt transmembrane orientation independent of the substituents attached along the scaffold. The construction of hydrogen-bonded chains along transmembrane rigid-rod scaffolds provided access to selective proton transport. Push−pull rods such as **1** with donors and acceptors at both ends gave ion channels that are activated by constructive macrodipole−potential interactions in polarized membranes (Figure 1). Cation−π interactions along π-basic *p*-oligophenyl rods were employed to build ligand-gated potassium transporters (i.e., **2**, Figure 1). The complementary anion−π slides were created with π-acidic naphthalenediimide (NDI) rods (e.g., **3**).[11] Perylenediimide (PDI) rods were made to combine active, photoinduced transport of electrons in one direction with passive anion antiport along anion−π slides (e.g., **4**).[12]

In artificial β-barrels, oligophenyl rods are used as 3D turns to roll the 2D β-sheets into the 3D barrels (e.g., **5**, Figure 1).[13] With hydrophobic amino acid residues at the outer and hydrophilic ones at the inner barrel surface, artificial β-barrels provided modular access to synthetic pores. Molecular recognition by these multifunctional pores was used to create catalytic pores and offered an ideal starting point for sensing applications.

The use of synthetic transport systems as sensors is somehow "natural" as our tongues and noses operate with responsive pores in lipid bilayer membranes. However, contrary to significant progress with bioengineered systems on the one hand and nonmembrane-based chemosensors on the other hand, the topic has attracted surprisingly little attention. To change this situation, we first focused on biosensing.[14,15] This term stands for the use of analyte-specific

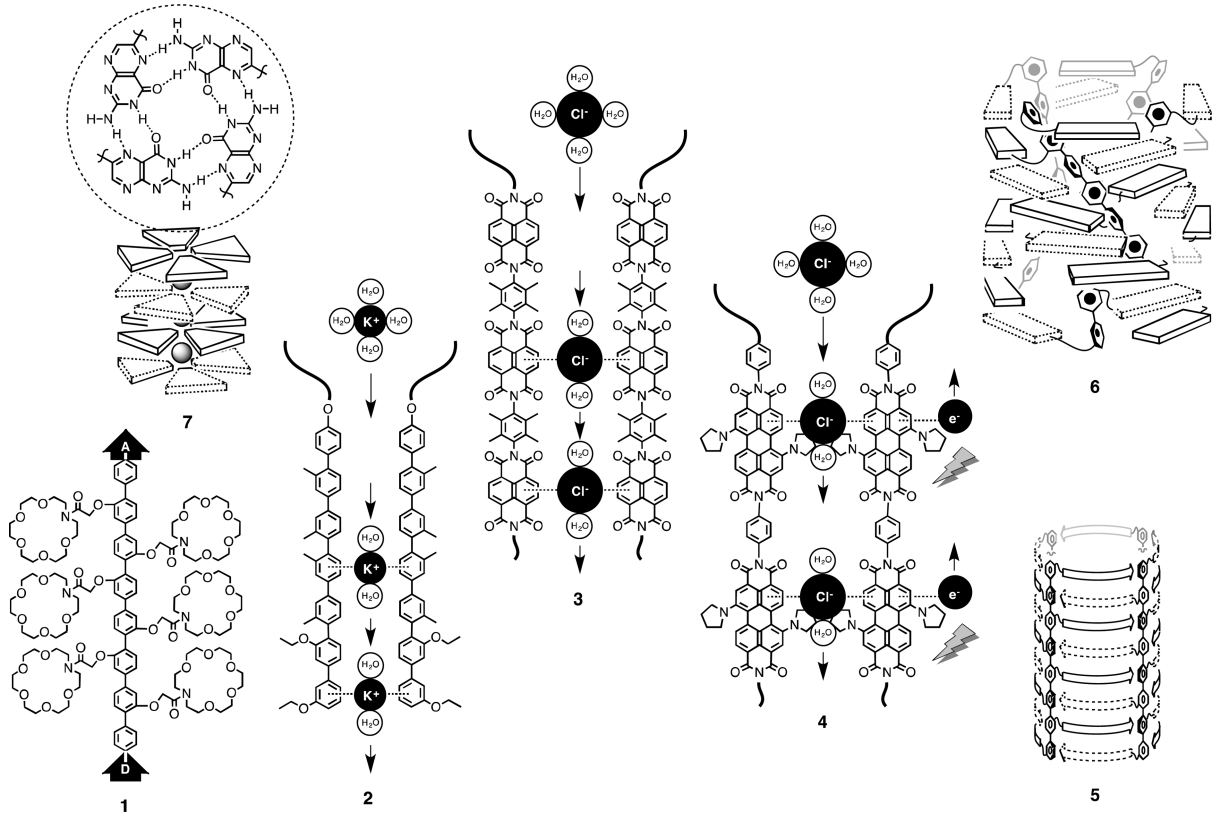

FIGURE 1. Classical motifs for transmembrane ion transport include push−pull rods **1**, cation−π slides **2**, anion−π slides **3**, anion−π photosystem **4**, artificial β-barrels **5**, and π−stack architectures **6** and **7**.

enzymes to generate the signal. Multifunctional pores that are activated or inactivated by substrates or products of the enzymatic signal generation were ideal for signal transduction. Biosensing with synthetic transport systems was exemplified with an artificial tongue,[15] additional analytes covered include inositol phosphates (phytate, IP_7),[16] polyphenols,[17] or cholesterol.[18]

"Immunosensing" with aptamers, the more accessible DNA counterpart of antibodies, was realized considering that the activity of DNA as counterion-activated cation transporter increases with increasing length.[19] Highly active supramolecular polymers of double-stranded helices were created with sticky ends for aptamers and their antiaptamers. Analyte binding then disassembles this active transporter into inactive single-stranded DNA fragments. This sensing strategy is attractive because it is universal and because, different to biosensing, the same molecule accounts for signal generation and signal transduction.

Differential sensors, that is, sensors that operate by pattern generation and pattern recognition, were the hardest to get with synthetic transport systems.[20] This was surprising because differential chemosensors have been successfully developed for almost any other method available, and because our nose works this way. Differential sensing is the only possibility to sense more than 10 000 odorants with ~350 olfactory receptors only. The problem with synthetic transport systems was pattern generation. This problem was solved with cations that contain one to six reactive hydrazides to capture ketone- or aldehyde-containing odorants in situ.[20] Patterns were then generated from the different ability of the obtained amphiphiles to activate DNA as cation transporter in fluorogenic vesicles. Pattern recognition by principal component analysis was successful for all analytes tested, including stereoisomers of muscone, citronellal, carvone, and cucumber aldehyde, and for perfumes.

The potential of synthetic transport systems as analytical tool to elaborate on otherwise less common interactions has been recognized only recently. However, interactions beyond the standard hydrogen bonding, ion pairing, or π-stacking (e.g., **6**, **7**) have been around for a while. Aromatic donor–acceptor interactions have appeared as π-clamps within artificial β-barrels for sensing applications[15,17] or as intercalators to untwist π-stacked photosystems **6** into ion channels (Figure 1).[21] Macrodipole–potential interactions in push–pull rods **1** have been used early on for voltage gating,[22−24] and cation–π interactions are of central interest in π-slides **2**. Membrane potentials have been applied to modulate molecular recognition[25,26] and catalysis.[27] The topic

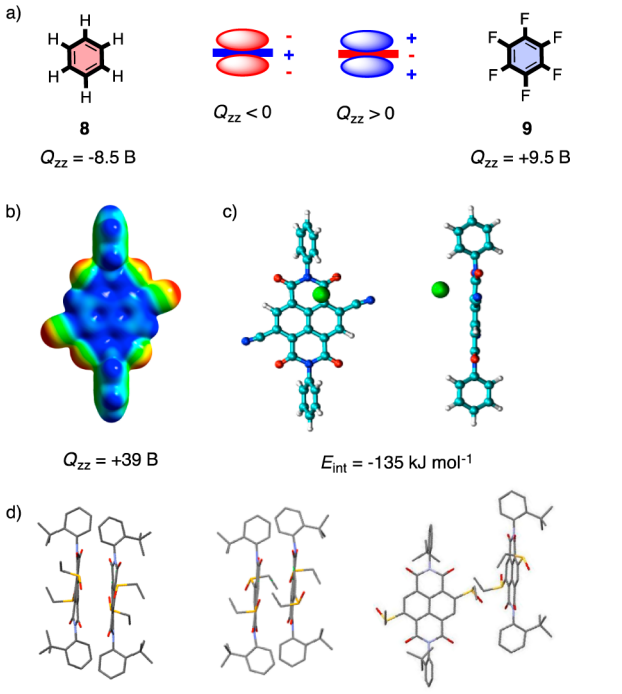

FIGURE 2. (a) For anion–π interactions to occur, the negative quadrupole moments Q_{zz} of π-basic aromatics has to be inverted. (b) Electrostatic potential surfaces and Q_{zz} of dicyano NDI **10** (red, electron-rich; blue, electron-poor); (c) chloride binding to **10** (compare Figure 3 for structure). Adapted from ref 28 with permission, 2010 Nature Publishing Group. (d) Crystal packing of (*M*)/(*P*)-**19** (left), (*M*)/(*P*)-**20** (middle), and (*P*)-**21** (right, obtained from (*M*)/(*P*)-**21**, compare Figure 5 for structures). Adapted from ref 30 with permission, 2012 Royal Society of Chemistry.

really came into focus when we wanted to see if anion–π interactions really account for the anion transport in anion–π slides such as **3** or **4**.[11,12] In the following, we will summarize the resulting studies on the use of synthetic transport systems to detect anion–π interactions,[28−31] halogen bonds,[31,32] and anion–macrodipole interactions[33] in action.

2. Anion–π Interactions

Most aromatic systems are π-basic, have a negative quadrupole moment $Q_{zz} < 0$, and can therefore attract cations (Figure 2a). Benzene **8**, for example, has a $Q_{zz} = -8.5$ Buckinghams (B). In cation–π slides **2**, we have used cation–π interactions along π-basic scaffolds to transport potassium cations across lipid bilayer membranes (Figure 1).[10] To attract anions rather than cations, the quadrupole moment perpendicular to the aromatic plane has to be inverted. This can be done; the most popular example for π-acids is hexafluorobenzene **9** with $Q_{zz} = +9.5$ B. In anion–π slides **3**, we have used NDIs because we found that their quadrupole moment is exceptionally high, in the range of TNT.[11]

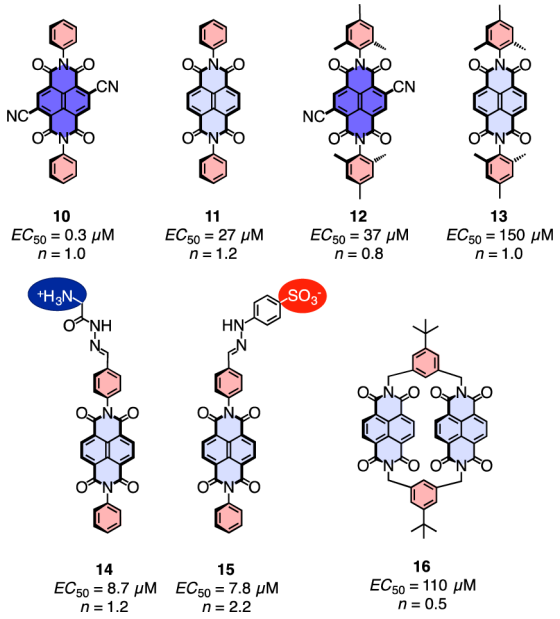

FIGURE 3. Structure of selected transporters with EC_{50}'s and Hill coefficients.

However, anion−π interactions are much less explored than cation−π interactions, difficult to confirm experimentally, and thus mostly ignored in the design of functional systems.[34−38] To verify that anion−π interactions really account for the activity of anion−π slides **3**, we started looking for model systems as simple as possible, with little left for anions to bind to except for a π-acidic surface. In the NDI **10**, the π-acidity is increased by two cyano substituents in the NDI core (Figure 3).[28] The electrostatic potential surface of **10** shows a totally blue surface for the naphthalene core, highly deficient of electrons (Figure 2b). An absolutely outstanding $Q_{zz} = +39$ B was the result.

In computational models, chloride binding was found to occur on the π-acidic surface, a bit off center and supported by C−H anion interactions with the peripheral phenyl group (Figure 2c). Decreasing π-acidity in **11** and increasing crowding of the active site in mesityl analogues **12** and **13** gradually reduced the binding energy $E_{int} = -135$ kJ mol^{-1} computed for **10** (Figures 2 and 3). The same trend was found in laser-induced tandem mass spectrometry (MS) fragmentation series for heterodimer complexes as well as in transport experiments in fluorogenic vesicles. The EC_{50} = 300 nM, that is the effective concentration needed to observe 50% activity in dose response curves, identified an unusually high activity for a transporter as small as **10**. Controls showed that nonspecific leakage does not contribute to the observed transport activity. The perfect match of computed binding energies, affinity series from tandem MS and transport activities was considered as convincing experimental evidence that anion−π interactions really account for the observed transport.

Hill coefficients deserve a general comment. They report on the stoichiometry as well as the stability of supramolecular transport systems.[39] Hill coefficients n are obtained from the Hill equation

$$Y \propto (c_M/EC_{50})^n$$

The equation describes all possible dose response curves, that is the dependence of transport activity Y on the concentration c_M of the transporter in monomeric form.

In its original meaning, the Hill coefficient n describes how many monomers are needed in the active structure. However, the Hill equation applies in this original meaning only as long as the concentration of the monomer is in excess,[40] that is for unstable supramolecules that exist only as a minority component together with an excess of inactive monomers. These unstable active structures, characterized by $n > 1$, are thus challenging to detect.

With the equilibrium shifting toward a supramolecular active structure, the monomer concentration becomes increasingly irrelevant. Instead, the concentration of the increasingly stable supramolecule enters into the Hill equation, which makes the Hill coefficient naturally go to one. Early on, this left us with the question how Hill analysis can identify such a stable supramolecule, characterized by $n = 1$. The answer was denaturation-assisted Hill analysis.[39] In this method, the stable supramolecule is first destabilized by chemical or thermal denaturation to artificially produce an excess of monomer, and then the dose response curve is recorded to reveal supramolecular nature and stoichiometry of the system of interest.

Applications of these lessons to the first generation of NDI transporters suggested that their active structure is either a monomer or a stable oligomer (Figure 3). The $n = 2.2$ found for NDIs **15** with a destabilizing negative charge already pointed toward supramolecular active structures. Hill coefficients up to $n = 7.4$ found in the second generation of NDI transporters implied the presence of at least octameric active structures (see below). Arguably, they are best considered as tetrameric bundles in both leaflets of the bilayer membrane. A particularly impressive example for the importance of a deep understanding of Hill coefficients will be given in the section on anion-macrodipole interactions.[33]

The anion selectivity topologies in fluorogenic vesicles depended strongly on the structure of the transporter. Weak selectivity with a general increase in activity with decreasing

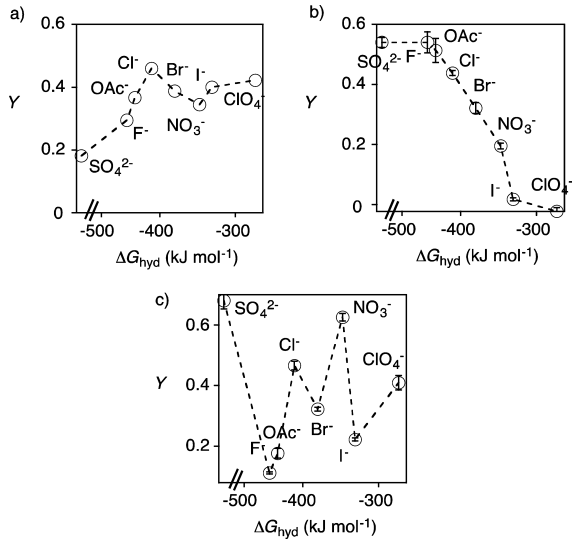

FIGURE 4. Anion selectivity topologies for (a) **14**, (b) **15**, and (c) **10**. Adapted from ref 28 with permission, 2010 Nature Publishing Group.

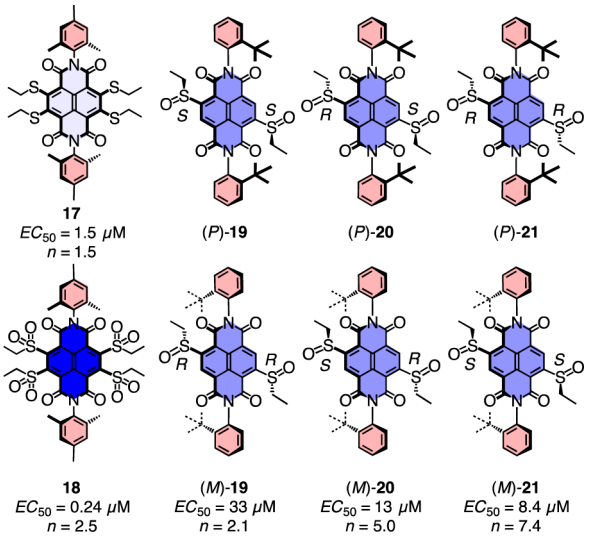

FIGURE 5. Structure of selected transporters with EC_{50}'s and Hill coefficients.

dehydration penalty was measured for NDI **14** (Figure 4a). This so-called Hofmeister topology is the least interesting outcome because it suggests that selectivity is determined by the cost of dehydration and contributions from binding to the transporter are less important. The origin of this boring selectivity topology was attributed to interference from nonspecific ion pairing near the π-acidic surface.

Replacement of the positive charge in **14** by a negative charge in **15** caused a dramatic change in the anion selectivity topology. The found anti-Hofmeister topology indicated that binding to the transporter overcompensates the cost of dehydration (Figure 4b). With increasing π-acidity and no nearby charges in **10**, the selectivity topology became independent of dehydration cost, fully determined by the binding to the transporter, with interesting preferences for chloride as well as oxyanions, particularly nitrate (Figure 4c). Anion$-\pi$ interactions enhanced by π,π-interactions with the planar oxyanion have been considered to account for this interesting selectivity.

Activities did not increase with dimeric NDIs **16**. Attempts to reach higher activities with increased $\pi-$acidity in the cyano series failed because the synthesis of the tetracyano NDIs with an outstanding $Q_{zz} = +55$ B (!) was not successful. Recent studies suggested that tetracyano NDIs are presumably too deficient in electrons to exist under ambient conditions.[41] To reach extreme π-acidities, an alternative approach was considered.[29] Four π-donating sulfide substituents were placed in the core of NDI **17** (Figure 5). Their oxidation to sulfones converted the π-donors into strong π-acceptors. The activity of the obtained NDI **18** was excellent, with $EC_{50} = 240$ nM slightly better than that of NDI **10** despite interfering methyl groups in the periphery.

The active suprastructures of the minimalist NDI transporters are unknown. Monomers are unlikely, also considering the relatively low binding energies around $E_{int} = -135$ kJ mol^{-1} (Figures 2 and 3). Poor activity of covalent dimers **16** does not exclude supramolecular active structures (Figure 3).[28] Their reduced activity could suggest that anions are bound too strongly to be released in time,[42] or that the dimer is too hydrophobic and precipitates before reaching the membrane. The self-assembly into supramolecular dimers was achieved with *tert*-butyl groups in *ortho*-position of the peripheral phenyl groups.[30] The most interesting results were obtained with stereoisomers **19**$-$**21** with two chiral sulfoxides in the core (Figure 5). Racemates (*M*)/(*P*)-**19** and (*M*)/(*P*)-**20** form heterodimers in solution and crystallize as racemates (Figure 2d). Enantiomers (*P*)-**21** and (*M*)-**21** crystallize as conglomerates because the two ethyl groups on the same side of the aromatic plane hinder face-to-face heterodimerization (Figure 2d). Highest activity found for racemates (*M*)/(*P*)-**21** suggested that active suprastructures of NDI transporters do not contain face-to-face π-stacks. Decreasing activity with decreasing Hill coefficients confirmed that unstable active structures are better than stable ones, and Hill coefficients up to $n = 7.4$ for (*M*)/(*P*)-**21** indicated the formation of at least octameric bundles as active structures. NDI architectures without π-stacks, including NDI nanotubes, have been reported before in different contexts.[43]

3. Halogen Bonds

Halogen bonds are the underrecognized counterpart of hydrogen bonds.[44$-$49] Like hydrogen bonds, they are directional

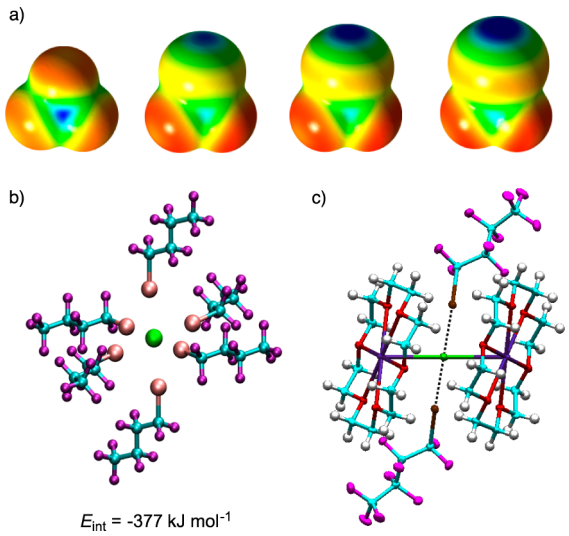

FIGURE 6. (a) Electrostatic potential surfaces of, left to right, CF_4, CF_3Cl, CF_3Br, and CF_3I (red, electron-rich; blue, electron-poor). (b) DFT model of chloride bound to six perfluoroiodobutane transporters **31** (compare Figure 7 for structure). (c) Crystal structure of chloride bound to two transporters **31** and potassium counterions bound to 18-crown-6. Adapted from ref 32 with permission, 2012 Nature Publishing Group.

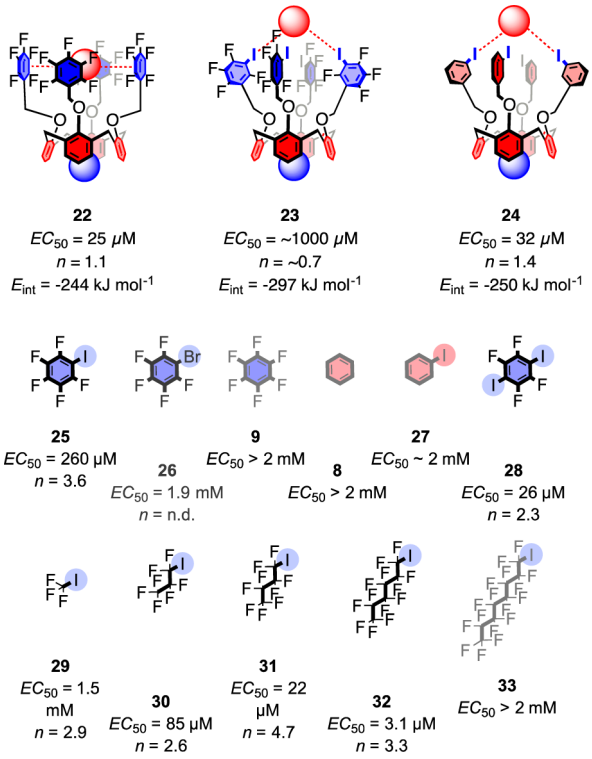

FIGURE 7. Structure of selected transporters with EC_{50}'s and Hill coefficients. **22**–**24**: Red spheres = anions, blue spheres = tetramethylammonium cations.

and strong. Different to hydrogen-bond donors, halogen-bond donors are hydrophobic. Halogen bonds originate from the localized positive charge density, the so-called σ-hole, that appears on top of a halogen atom from which electrons are being pulled away by strongly withdrawing substituents (see blue spot in Figure 6a). Halogen bonds are strongest with iodines but occur also with electron-deficient bromines and chlorines.

Similar to anion–π interactions, halogen bonds are attractive in theory, confirmed to exist in the solid state and in solution but just at the beginning to be explored in depth for molecular recognition, ion binding, catalysis, and other activities. Considering their unique combination of strength and directionality with hydrophobicity, synthetic transport systems appeared ideal to further expand the usefulness of halogen bonds for the creation of function. Calix[4]arene scaffolds were considered first (Figure 7).[31] The binding of tetramethylammonium cations to the macrocycle was envisioned to support anion binding to arene arrays above the macrocycle. In calixarene **22**, the pentafluorophenyl arrays gave with $EC_{50} = 25$ μM reasonable activities in support of operational anion–π interactions. Ongoing studies with complementary calix[4]pyrroles from the Ballester group in Tarragona further corroborate the general ability of anion–π interactions to mediate anion transport across lipid bilayer membranes (A. Vargas Jentzsch, S. Matile, P. Ballester, unpublished results).

Replacement of one fluorine per phenyl in **22** with an iodine in *meta*-position in **23** reduced transport activity to $EC_{50} \sim 1$ mM. However, computational models confirmed that the halogen bonds in **23** increase rather than decrease the anion binding energies. The inhibition of transport by excessive binding is understood theoretically,[42] dimeric NDI **16** could loose activity for the same reason (Figure 3). This explanation suggested that weakening of anion binding in **23** could restore activity. One way to do this was to replace the withdrawing fluorines in **23** by hydrogens in **24**. The result was convincing, activities went up as computed binding energies went down, both ending up near those of **22**. However, the most drastic way to weaken anion binding in **23** was to forget about the entire calixarene and try just pentafluoroiodobenzene **25** instead.[32] Quite remarkably, activities increased about four times to $EC_{50} = 260$ μM, together with Hill coefficients going up to $n = 3.6$. Activity vanished with weaker halogen-bond donors in pentafluorobromobenzene **26** and iodobenzene **27**, anion–π and cation–π controls **8** and **9** were inactive. High activity with perfluorinated diiodobenzene **28** implied the presence of higher-order active structures.

In the perfluoroiodoalkane series **29**–**33**, linear chains of intermediate length were best (Figure 7). A maximal

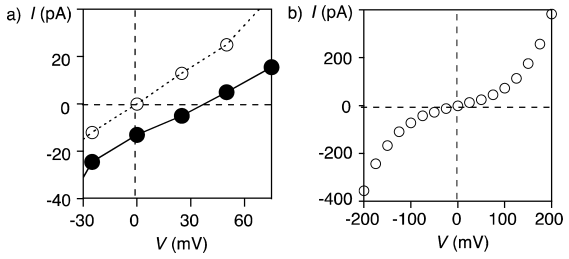

FIGURE 8. (a) Ion selectivity and (b) voltage dependence of transporter **25** in planar bilayer conductance experiments. (a) 2 M KCl *cis* and *trans* (empty circles) or 2 M KCl *cis* and 0.25 M KCl in *trans* (filled circles). (b) 2 M KCl *cis* and *trans*. Adapted from ref 32 with permission, 2012 Nature Publishing Group.

$EC_{50} = 3.1\ \mu M$ was recorded for **32**. Shorter tails remained detectable down to the single-carbon transporter **29**, whereas longer ones were inactive because of the sharp onset of competing self-assembly. Trifluoroiodomethane **29**, by definition the smallest possible organic anion transporter, is a gas with a boiling point of −22 °C. Anion transport could be turned on by simply bubbling the gas through an aqueous suspension of vesicles. Activities increased with increasing bubbling time. This quite remarkable evidence for transport with maximal atom efficiency underscores the power of halogen bonds compared to hydrogen bonds for transport: Both are directional and strong, but halogen-bond donors are hydrophobic, whereas hydrogen-bond donors are hydrophilic.

In fluorogenic vesicles, anion selectivities with anti-Hofmeister topologies were observed. The validity of these results in vesicles was confirmed with conductance experiments in planar lipid bilayers. Application of a KCl gradient across the membrane generated negative currents flowing at zero voltage (Figure 8a, filled circles). The reversal potentials needed to stop these currents from flowing corresponded to permeability ratios of up to $P_{Cl/K} = 37$. This is very high, biological chloride channels have $P_{Cl/K} \sim 5$. Intriguingly, anion transport with minimalist halogen-bond donors violated Ohm's law (Figure 8b). Exponential curve fit of the nonlinear voltage dependence gave gating charges $z_g \sim 0.4$. This result suggested that anion binding and release are faster than transport, and that direct acceleration of transport, that is true current rectification, accounts for this significant voltage dependence.

Hill coefficients up to $n = 4.7$ were consistent with the binding of five or six halogen-bond donors around one hydroxide or chloride anion (Figure 6b). Crystal structures from the groups of Metrangolo and Resnati in Milan confirmed the occurrence of halogen bonds between two transporters **31** and a chloride, additional binding sites were obscured by counterions trapped within bulky crown ethers (Figure 6c). Viewed together, these results point toward an active structure with multiple minimalist halogen bond donors encapsulating the anion within a hydrophobic shell (Figure 6b). This active structure is stable enough to compensate for dehydration penalty but unstable and labile enough to afford high Hill coefficients and voltage gating, respectively, and to avoid inhibition of transport (compare **23** and **16**).

4. Anion−Macrodipole Interactions

Compared to transport with anion−π interactions and halogen bonds, transport with anion−macrodipole interactions is different for several reasons. On the one hand, they do not expand the number of interactions available to achieve function beyond precedence in biology. Quite the contrary, interactions between the focal point of positive and negative ends of the macrodipoles of bundled α-helices and anions and cations, respectively, play a crucial role in biological potassium and chloride channels.[1−3,33] On the other hand, synthetic transport systems that operate with anion−macrodipole interactions are necessarily big, experimental evidence for anion-macrodipole interactions cannot be "nailed down" by removing all possible contributions from other sources.

We entered the topic with peptide-urea nanotubes from the Guichard group in Bordeaux.[33] Solution studies and crystal structures demonstrated that macrocycle **34** self-assembles into nanotubes **35** (Figure 9b).[50] Intermolecular hydrogen bonding, mediated by a molecule of water between two macrocycles, orients all carbonyl dipoles uniformly and thus produces a strong macrodipole. Macrocycle **36** self-assembles into nanotubes **37** that have similar global structure but no macrodipole. Crystal structures of the alkyl homologue of **36** show dimers with antiparallel carbonyls that self-assemble on top of each other with the support of two molecules of water (Figure 9a).

Anion binding at the positive end of the macrodipole of nanotube **35** should thus be supported by anion-macrodipole interactions, whereas nanotube **37** should fail to operate with anion-macrodipole interactions. In fluorogenic vesicles, macrocycles **34** and **36** were active as anion transporters. The anion selectivity of **36** roughly followed a Hofmeister topology (Figure 10b), whereas **34** gave an anti-Hofmeister topology (Figure 10a). This nice difference supported that anion binding to nanotube **35** with a strong macrodipole overcompensates dehydration penalty and dominates transport, whereas macrodipole-free nanotube **37** does not contribute much to selectivity.

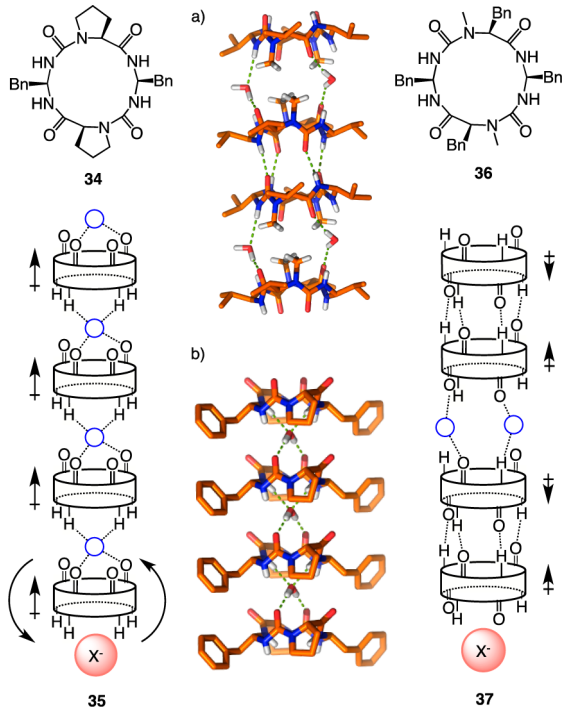

FIGURE 9. Self-assembly of **34** and **36** into nanotubes **35** and **37**. (a) Crystal structure of **37** (alkyl instead of Bn substituents); (b) crystal structure of **35**. Adapted from ref 50 with permission, 2010 Royal Society of Chemistry.

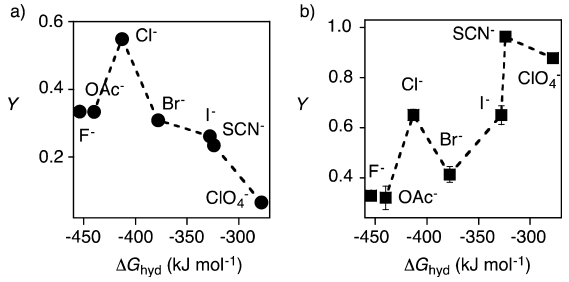

FIGURE 10. Anion selectivity topology of macrocycles **34** (a) and **36** (b). Adapted with permission from ref 33. Copyright 2009 American Chemical Society.

The interior of nanotube **35** is too small to let anions pass through. This left us with the question how anions could move across the membrane after the likely binding to the positive end of the macrodipole. A conceivable explanation was that the first macrocycle with the bound anion on one side and water on the other side would rotate around its equatorial axis to make anion and water change place (Figure 9). Then, the second macrocycle would rotate to move the anion forward, and so on until the anion is released on the other side and all macrocycles in the nanotube are back in their resting state, ready to bind and translocate the next anion. This so far fully speculative mechanism is reminiscent of the rotational translocation along a Jacobs ladder. Driven by a transmembrane gradient, the Jacobs ladder would operate with a subtle balance between losses in macrodipole and gains in hydrogen bonding to anions sandwiched between two antiparallel macrocycles, and vice versa.

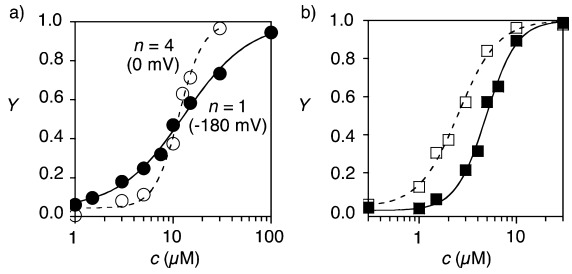

FIGURE 11. Dose response curve of **34** (a) and **36** (b) without (empty symbols) and with inside negative membrane potentials (filled symbols). Adapted with permission from ref 33. Copyright 2009 American Chemical Society.

To elaborate on the presence and relevance of the macrodipole for anion binding and transport, activities in polarized vesicles were determined. For dipole-free nanotubes **37**, EC_{50}'s increased with increasing membrane potentials, whereas Hill coefficients remained constant (Figure 11b). This change can be interpreted by a destruction of the active structure upon alignment of the dipoles of the macrocycles with the potential. In clear contrast, activities of nanotube **35** remained constant with increasing membranes potentials, whereas Hill coefficients decreased from $n = 4$ to $n = 1$ (Figure 11a). This change suggested that the active structure is stabilized by constructive potential–macrodipole interactions. In other words, decreasing Hill coefficients with increasing membrane potentials was consistent with the existence and functional relevance of an active structure with a strong macrodipole, that is, nanotube **35**.

5. Summary and Outlook

Over the years, the focus in the field of synthetic transport systems has gradually shifted from basic can-do curiosity toward applications in materials sciences (sensing, photosystems), biology (cellular uptake), and medicine. In this Account, an emerging new application of synthetic transport systems has been summarized, that is their possible use as analytical tool to determine the functional relevance of interactions that are otherwise difficult to detect. Examples covered are anion–π interactions, halogen bonds and anion macrodipole interactions.

The summarized studies illustrate that the interpretation of results with synthetic transport systems can be quite speculative. Thoughtful design of experiments is essential to find meaningful answers. For instance, the development

of structurally similar controls that show dichotomic behavior is of highest importance. Nanotubes **35** and **37** are nice examples for dichotomic partners. Hill coefficients have emerged as solid source of information on both cooperativity as well as stability. Methods have been developed to understand the most demanding situation with stable active supramolecules with $n = 1$ (i.e., denaturation-assisted Hill analysis).[39] The message that structure determination of unstable active supramolecules with $n > 1$ has to be done with utmost caution has been understood (because they are minority components).

The lessons learned with anion−π interactions, halogen bonds, and anion−macrodipole interactions are very basic. As a result, their possible applications are very general. Applications to the established topics mentioned above are obvious. Applications to molecular recognition are less meaningful because the interactions of interest are exactly the interactions that are too weak to detect and used easily in molecular recognition, and because the tight binding needed in molecular recognition often inhibits transport. Cyclophane **16** and calixarene **23** are telling examples for this general rule.

Applications to catalysis, in contrast, are most enticing. As for transport, weak interactions are best for catalysis. Evidence for the transport of anions implies that anionic transition states should be stabilizable in the same way. Whereas catalysis with halogen bonds is slowly taking momentum,[49] catalysis with anion−macrodipole interactions receives less attention and catalysis with anion−π interactions remains to be realized. This is surprising considering the importance of cation−π interactions to stabilize carbocation intermediates, particularly in the biosynthesis of terpenoids and steroids.[51,52] The holy grail is the combination of transport and catalysis, that is, translocation and transformation. One isolate example on catalytic pores that operate with standard ion pairing exists and justifies highest expectations for the expansion toward anion−π interactions, halogen bonds, and anion−macrodipole interactions (transition-state stabilization $\Delta G = -56$ kJ mol^{-1}, voltage dependence, etc.).[27] We do not know what we will learn from combining transport and catalysis. All we know is that, like all good research on synthetic transport systems, it will not be boring.

We warmly thank all present and past co-workers and collaborators that contributed to this research, particularly the groups of Christoph Schalley (Berlin), Marcel Mayor (Basel), Gilles Guichard (Bordeaux), Pablo Ballester (Tarragona), and Pierangelo Metrangolo and Giuseppe Resnati (Milan). The University of Geneva and the Swiss Center for Scientific Computing are acknowledged for providing the computer resources. For financial support, we thank the University of Geneva, the European Research Council (ERC Advanced Investigator), the National Centre of Competence in Research (NCCR) Chemical Biology, and the Swiss NSF.

Note Added in Proof. For high transport activity with halogen bonds, we felt that the cyclic oligomers **23** (EC_{50} = 1 mM, Figure 7)[31] would have to be unrolled into linear ones that would be compatible with cooperative anion hopping along transmembrane arrays of halogen-bond donors. The first results with the classical *p*-oligophenyl scaffold[10] have just been published: An unprecedented cooperativity coefficient $m = 3.37$ for increasing oligomer length, far beyond the $1 < m < 2$ for standard multivalency, leads to an $EC_{50} = 110$ nM for the most active octamer **38** (Figure 12).[53] The deiodinated controls for anion-π interactions are also quite active ($m = 2.13$, $EC_{50}^{MAX} = 1.3$ μM).

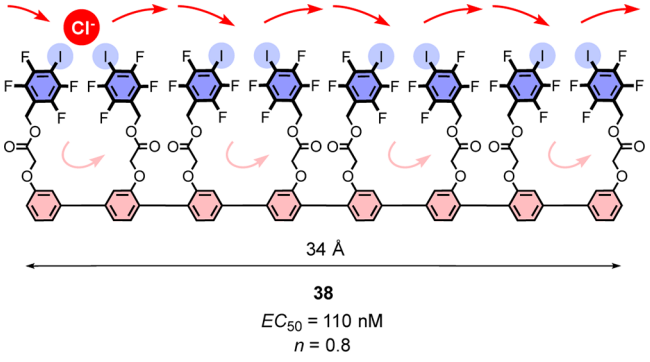

FIGURE 12. Transmembrane halogen-bonding cascades.

BIOGRAPHICAL INFORMATION

Andreas Vargas Jentzsch was born in Cochabamba, Bolivia, on January 12, 1984. He was educated at the University of Geneva (M.Sc., 2009). In 2009, he started a Ph.D. under the supervision of Professor Stefan Matile at the University of Geneva.

Andreas Hennig studied Chemistry at the TU Braunschweig (Diploma, 2004) and the Jacobs University Bremen (Ph.D., 2007). After a postdoctoral stay with Professor Stefan Matile at the University of Geneva (2007−2009), he currently holds a position as research scientist at the Federal Institute for Materials Research and Testing (BAM) in Berlin. His research expertise focuses on spectroscopic studies of functional supramolecular systems and the development of nanobiotechnological applications.

Jiri Mareda received both his Diploma (1975) and Ph.D. (1980) from the University of Geneva for research with Professors Charles W. Jefford and Ulrich Burger. He then joined Ken Houk for a postdoctoral stay (1980−1983) before returning to Geneva, where he joined the Faculty to focus on computational chemistry in a broader sense.

Stefan Matile was born in Zurich, Switzerland, on July 13, 1963. He was educated at the University of Zurich (Ph.D., 1994) and Columbia University in New York (Postdoc). He joined the faculty at

Georgetown University in Washington, D.C. in 1996 and moved to the University of Geneva, Switzerland, in 1999, where he is currently Full Professor of Organic Chemistry, ERC Advanced Investigator and Project Leader in the NCCR Chemical Biology.

FOOTNOTES

*To whom correspondence should be addressed. E-mail: stefan.matile@unige.ch.
The authors declare no competing financial interest.

REFERENCES

1 Matile, S.; Som, A.; Sordé, N. Recent Synthetic Ion Channels and Pores. *Tetrahedron* **2004**, *60*, 6405–6435.

2 Sisson, A. L.; Shah, M. R.; Bhosale, S.; Matile, S. Synthetic Ion Channels and Pores (2004−2005). *Chem. Soc. Rev.* **2006**, *35*, 1269–1286.

3 Matile, S.; Vargas Jentzsch, A.; Fin, A.; Montenegro, J. Recent Synthetic Transport Systems. *Chem. Soc. Rev.* **2011**, *40*, 2453–2474.

4 Chui, J. K.; Fyles, T. M. Ionic Conductance of Synthetic Channels: Analysis, Lessons, and Recommendations. *Chem. Soc. Rev.* **2012**, *41*, 148–175.

5 Davis, J. T.; Okunola, O.; Quesada, R. Recent Advances in the Transmembrane Transport of Anions. *Chem. Soc. Rev.* **2010**, *39*, 3843–3862.

6 Davis, A. P.; Sheppard, D. N.; Smith, B. D. Development of Synthetic Membrane Transporters for Anions. *Chem. Soc. Rev.* **2007**, *36*, 348–357.

7 Gale, P. A. From Anion Receptors to Transporters. *Acc. Chem. Res.* **2011**, *44*, 216–226.

8 Gokel, G. W.; Barkey, N. Transport of Chloride Ion Through Phospholipid Bilayers Mediated by Synthetic Ionophores. *New J. Chem.* **2009**, *33*, 947–963.

9 Fyles, T. M.; Matile, S., Eds. Synthetic Transport Systems in Lipid Bilayer Membranes. *Acc. Chem. Res.*, this issue.

10 Sakai, N.; Mareda, J.; Matile, S. Rigid-Rod Molecules in Biomembrane Models: From Hydrogen-Bonded Chains to Synthetic Multifunctional Pores. *Acc. Chem. Res.* **2005**, *38*, 79–87.

11 Gorteau, V.; Bollot, G.; Mareda, J.; Perez-Velasco, A.; Matile, S. Rigid Oligonaphthalenediimide Rods as Transmembrane Anion−π Slides. *J. Am. Chem. Soc.* **2006**, *128*, 14788–14789.

12 Perez-Velasco, A.; Gorteau, V.; Matile, S. Rigid Oligoperylenediimide Rods: Anion−π Slides with Photosynthetic Activity. *Angew. Chem., Int. Ed.* **2008**, *47*, 921–923.

13 Sakai, N.; Mareda, J.; Matile, S. Artificial β-Barrels. *Acc. Chem. Res.* **2008**, *41*, 1354–1365.

14 Das, G.; Talukdar, P.; Matile, S. Fluorometric Detection of Enzyme Activity with Synthetic Supramolecular Pores. *Science* **2002**, *298*, 1600–1602.

15 Litvinchuk, S.; Tanaka, H.; Miyatake, T.; Pasini, D.; Tanaka, T.; Bollot, G.; Mareda, J.; Matile, S. Synthetic Pores with Reactive Signal Amplifiers as Artificial Tongues. *Nat. Mater.* **2007**, *6*, 576–580.

16 Butterfield, S. M.; Tran, D.-H.; Zhang, H.; Prestwich, G. D.; Matile, S. Fluorometric Detection of Inositol Phosphates and the Activity of their Enzymes with Synthetic Pores: Discrimination of IP_7 and IP_6 and Phytate Sensing in Complex Matrices. *J. Am. Chem. Soc.* **2008**, *130*, 3270–3271.

17 Hagihara, S.; Tanaka, H.; Matile, S. Boronic Acid Converters for Reactive Hydrazide Amplifiers: Polyphenol Sensing in Green Tea with Synthetic Pores. *J. Am. Chem. Soc.* **2008**, *130*, 5656–5657.

18 Butterfield, S. M.; Miyatake, T.; Matile, S. Amplifier-Mediated Activation of Cell Penetrating Peptides with Steroids: Multifunctional Anion Transporters for Fluorogenic Cholesterol Sensing in Eggs and Blood. *Angew. Chem., Int. Ed.* **2009**, *48*, 325–328.

19 Takeuchi, T.; Matile, S. DNA Aptamers as Analyte-Responsive Cation Transporters in Fluorogenic Vesicles: Signal Amplification by Supramolecular Polymerization. *J. Am. Chem. Soc.* **2009**, *131*, 18048–18049.

20 Takeuchi, T.; Montenegro, J.; Hennig, A.; Matile, S. Pattern Generation with Synthetic Sensing Systems in Lipid Bilayer Membranes. *Chem. Sci.* **2011**, *2*, 303–307.

21 Bhosale, S.; Sisson, A. L.; Talukdar, P.; Fürstenberg, A.; Banerji, N.; Vauthey, E.; Bollot, G.; Mareda, J.; Röger, C.; Würthner, F.; Sakai, N.; Matile, S. Photoproduction of Proton Gradients with π-Stacked Fluorophore Scaffolds in Lipid Bilayers. *Science* **2006**, *313*, 84–86.

22 Winum, J.-Y.; Matile, S. Rigid Push-Pull Oligo(p-Phenylene) Rods: Depolarization of Bilayer Membranes with Negative Membrane Potential. *J. Am. Chem. Soc.* **1999**, *121*, 7961–7962.

23 Sakai, N.; Matile, S. Recognition of Polarized Bilayer Membranes by p-Oligophenyl Ion Channels: From Push-Pull Rods to Push-Pull β-Barrels. *J. Am. Chem. Soc.* **2002**, *124*, 1184–1185.

24 Sakai, N.; Houdebert, D.; Matile, S. Voltage-Dependent Formation of Anion Channels by Synthetic Rigid-Rod Push-Pull β-Barrels. *Chem.—Eur. J.* **2003**, *9*, 223–232.

25 Baudry, Y.; Pasini, D.; Nishihara, M.; Sakai, N.; Matile, S. The Depth of Molecular Recognition: Voltage-Sensitive Blockage of Synthetic Multifunctional Pores with Refined Architecture. *Chem. Commun.* **2005**, *40*, 4798–4800.

26 Sakai, N.; Baumeister, B.; Matile, S. Transmembrane B-DNA. *ChemBioChem* **2000**, *1*, 123–125.

27 Sakai, N.; Sordé, N.; Matile, S. Synthetic Catalytic Pores. *J. Am. Chem. Soc.* **2003**, *125*, 7776–7777.

28 Dawson, R. E.; Hennig, A.; Weimann, D. P.; Emery, D.; Ravikumar, V.; Montenegro, J.; Takeuchi, T.; Gabutti, S.; Mayor, M.; Mareda, J.; Schalley, C. A.; Matile, S. Experimental Evidence for the Functional Relevance of Anion−π Interactions. *Nat. Chem.* **2010**, *2*, 533–538.

29 Misek, J.; Vargas Jentzsch, A.; Sakurai, S.; Emery, D.; Mareda, J.; Matile, S. A Chiral and Colorful Redox Switch: Enhanced π Acidity in Action. *Angew. Chem., Int. Ed.* **2010**, *49*, 7680–7683.

30 Lin, N.-T.; Vargas Jentzsch, A.; Guénée, L.; Neudörfl, J.-M.; Aziz, S.; Berkessel, A.; Orentas, E.; Sakai, N.; Matile, S. Enantioselective Self-Sorting on Planar, π-Acidic Surfaces of Anion−π Transporters. *Chem. Sci.* **2012**, *3*, 1121–1127.

31 Vargas Jentzsch, A.; Emery, D.; Mareda, J.; Metrangolo, P.; Resnati, G.; Matile, S. Ditopic Ion Transport Systems: Anion−π Interactions and Halogen Bonds at Work. *Angew. Chem., Int. Ed.* **2011**, *50*, 11675–11678.

32 Vargas Jentzsch, A.; Emery, D.; Mareda, J.; Nayak, S. K.; Metrangolo, P.; Resnati, G.; Sakai, N.; Matile, S. Transmembrane Anion Transport Mediated by Halogen-Bond Donors. *Nat. Commun.* **2012**, *3*, 905.

33 Hennig, A.; Fischer, L.; Guichard, G.; Matile, S. Anion-Macrodipole Interactions: Self-Assembling, Macrocyclic Oligourea/Amide Anion Transporters that Respond to Membrane Polarization. *J. Am. Chem. Soc.* **2009**, *131*, 16889–16895.

34 Frontera, A.; Gamez, P.; Mascal, M.; Mooibroek, T. J.; Reedijk, J. Putting Anion−π Interactions Into Perspective. *Angew. Chem., Int. Ed.* **2011**, *50*, 9564–9583.

35 Schottel, B. L.; Chifotides, H. T.; Dunbar, K. R. Anion−π Interactions. *Chem. Soc. Rev.* **2008**, *37*, 68–83.

36 Ballester, P. Experimental Quantification of Anion−π Interactions in Solution Using Neutral Host-Guest Model Systems. *Acc. Chem. Res.*, in press.

37 Cadman, C. J.; Croft, A. K. Anion−π Interactions Influence pK_a Values. *Beilstein J. Org. Chem.* **2011**, *7*, 320–328.

38 Giese, M.; Albrecht, M.; Wiemer, K.; Kubik, G.; Valkonen, A.; Rissanen, K. Weak Intermolecular Anion−π Interactions in Pentafluorobenzyl-Substituted Ammonium Betaines. *Eur. J. Inorg. Chem.* **2012**, 2995–2999.

39 Bhosale, S.; Matile, S. A Simple Method to Identify Supramolecules in Action: Hill Coefficients for Exergonic Self-Assembly. *Chirality* **2006**, *18*, 849–856.

40 Stadler, E.; Dedek, P.; Yamashita, K.; Regen, S. L.; Amphotericin, B. Mimics: A Sterol-Based Ionophore. *J. Am. Chem. Soc.* **1994**, *116*, 6677–6682.

41 Chang, J.; Ye, Q.; Huang, K.-W.; Zhang, J.; Chen, Z.-K.; Wu, J.; Chi, C. Stepwise Cyanation of Naphthalene Diimide for n-Channel Field-Effect Transistors. *Org. Lett.* **2012**, *14*, 2964–2967.

42 Behr, J.-P.; Kirch, M.; Lehn, J.-M. Carrier-Mediated Transport Through Bulk Liquid Membranes: Dependence of Transport Rates and Selectivity on Carrier Properties in a Diffusion-Limited Process. *J. Am. Chem. Soc.* **1985**, *107*, 241–246.

43 Ponnuswamy, N.; Pantoş, G. D.; Smulders, M. M. J.; Sanders, J. M. K. Thermodynamics of Supramolecular Naphthalenediimide Nanotube Formation: The Influence of Solvents, Side Chains, and Guest Templates. *J. Am. Chem. Soc.* **2012**, *134*, 566–573.

44 Cavallo, G.; Metrangolo, P.; Pilati, T.; Resnati, G.; Sansotera, M.; Terraneo, G. Halogen Bonding: A General Route in Anion Recognition and Coordination. *Chem. Soc. Rev.* **2010**, *39*, 3772–3783.

45 Zapata, F.; Caballero, A.; White, N. G.; Claridge, T. D. W.; Costa, P. J.; Félix, V.; Beer, P. D. Fluorescent Charge-Assisted Halogen-Bonding Macrocyclic Halo-Imidazolium Receptors for Anion Recognition and Sensing in Aqueous Media. *J. Am. Chem. Soc.* **2012**, *134*, 11533–11541.

46 Chudzinski, M. G.; McClary, C. A.; Taylor, M. S. Anion Receptors Composed of Hydrogen- and Halogen-Bond Donor Groups: Modulating Selectivity with Combinations of Distinct Noncovalent Interactions. *J. Am. Chem. Soc.* **2011**, *113*, 10559–10567.

47 Hardegger, L. A.; Kuhn, B.; Spinnler, B.; Anselm, L.; Ecabert, R.; Stihle, M.; Gsell, B.; Thoma, R.; Diez, J.; Benz, J.; Plancher, J. M.; Hartmann, G.; Banner, D. W.; Haap, W.; Diederich, F. Systematic Investigation of Halogen Bonding in Protein-Ligand Interactions. *Angew. Chem., Int. Ed.* **2011**, *50*, 314–318.

48 Auffinger, P.; Hays, F. A.; Westhof, E.; Ho, P. S. Halogen Bonds in Biological Molecules. *Proc. Natl. Acad. Sci. U.S.A.* **2004**, *101*, 16789–16794.

49 Bruckmann, A.; Pena, M. A.; Bolm, C. Organocatalysis through Halogen-Bond Activation. *Synlett* **2008**, *6*, 900–902.

50 Fischer, L.; Guichard, G. Folding and Self-Assembly of Aromatic and Aliphatic Urea Oligomers: Towards Connecting Structure and Function. *Org. Biomol. Chem.* **2010**, *8*, 3101–3117.

51 Ma, J. C.; Dougherty, D. A. The Cation−π Interaction. *Chem. Rev.* **1997**, *97*, 1303–1324.

52 Knowles, R. R.; Lin, S.; Jacobsen, E. N. Enantioselective Thiourea-Catalyzed Cationic Polycyclizations. *J. Am. Chem. Soc.* **2010**, *132*, 5030–5032.

53 Vargas Jentzsch, A.; Matile, S. Transmembrane Halogen-Bonding Cascades. *J. Am. Chem. Soc.* **2013**, DOI:10.1021/ja4013276.